Metallaborane Chemistry. Part 12.[1] Electron Hyper-deficient Carbametallaboranes containing Iron–Iron, Iron–Cobalt, and Iron–Platinum Connectivities: Molecular and Crystal Structure of $[CoFe(Me_4C_4B_8H_8)(PEt_3)_2]$

By **Geoffrey K. Barker, Maria P. Garcia, Michael Green,** and **F. Gordon A. Stone,** Department of Inorganic Chemistry, The University, Bristol BS8 1TS
Alan J. Welch, Department of Chemistry, University of Edinburgh, Edinburgh EH9 3JJ

The dihydridocarbaferraborane $[FeH_2(2,3\text{-}Me_2\text{-}2,3\text{-}C_2B_4H_4)_2]$ reacts with $[Co(PEt_3)_4]$, $[Pt_2(\mu\text{-cod})(PEt_3)_4]$ (cod = cyclo-octa-1,5-diene), and $[Fe(cod)(\eta\text{-}C_5H_5)]$ to afford, respectively, the dimetallic species $[CoFe(Me_4C_4B_8H_8)(PEt_3)_2]$, $[FePt(Me_4C_4B_8H_8)(PEt_3)_2]$, and $[Fe_2(Me_4C_4B_8H_8)(\eta\text{-}C_5H_5)]$, each of which features a metal–metal connectivity. An *X*-ray diffraction study of the iron–cobalt molecule shows that it belongs to the structural family involving two pentagonal bipyramids fused about a common iron apical vertex and sharing a double-capping BH function. Crystals are orthorhombic, space group $P2_12_12_1$ with a = 16.533(5), b = 11.012(2), c = 16.279(3) Å, and four molecules per unit cell. Using 3 496 amplitudes recorded on a four-circle diffractometer at 291 ± 1 K the structure has been refined to R 0.043. The Co–Fe distance is 2.5300(8) Å; 0.05 Å longer than that in $[CoFe(Me_4C_4B_8H_8)(\eta\text{-}C_5H_5)]$.

ONE of the most important synthetic routes to carbametallaborane polyhedra, developed over the last decade, is the so-called direct insertion reaction. On a simple basis this may be viewed as the oxidative addition of a low-valent metal species (nucleophile) to a borane or heteroborane cage (electron deficient in the classical sense). In this manner expansion of the polyhedron to include the metal atom occurs. In the earlier papers of this series we have shown how metal fragments ML_2 (M = Ni, Pd, or Pt; L = PR_3 or CNR, where R = alkyl or aryl) are inserted into a variety of *closo*-,[1-4] *nido*-,[5,6] and *arachno*-polyhedra,[7] and in recent communications we have extended the principle of direct insertion to include cobalt,[8-10] rhodium,[10] and iron [11] nucleophiles. A consistent feature of this synthetic approach is that the carbametallaboranes formed are obtained in relatively high yields under mild conditions.

Recently, Grimes and co-workers [12] reported that u.v. irradiation of $[Co(CO)_2(\eta\text{-}C_5H_5)]$ in the presence of the dihydridocarbaferraborane $[FeH_2(2,3\text{-}Me_2\text{-}2,3\text{-}C_2B_4H_4)_2]$ led to the apparent elimination of molecular hydrogen and the direct insertion of a $Co(\eta\text{-}C_5H_5)$ fragment to afford in low yield (11%) the electron hyper-deficient species $[CoFe(Me_4C_4B_8H_8)(\eta\text{-}C_5H_5)]$. The latter was shown by an *X*-ray diffraction study to contain a double-capping BH function, and a direct Co–Fe interaction. This reaction may be viewed as an example of the direct insertion route where a photochemically generated $Co(CO)(\eta\text{-}C_5H_5)$ fragment oxidatively inserts into a *closo*-cage with either concomitant or subsequent elimination of H_2 and CO.

With this possible relationship in mind we have examined the reaction of the nucleophilic metal species $[Co(PEt_3)_4]$, $[Pt_2(\mu\text{-cod})(PEt_3)_4]$, and $[Fe(cod)(\eta\text{-}C_5H_5)]$ (cod = cyclo-octa-1,5-diene) with $[FeH_2(2,3\text{-}Me_2\text{-}2,3\text{-}C_2B_4H_4)_2]$,[13,14] and have isolated new complexes containing Fe–Fe, Fe–Co, and Fe–Pt bonds.

EXPERIMENTAL

Nuclear magnetic resonance spectra, measured at room temperature in $[^2H_8]$toluene unless otherwise stated, were recorded on JEOL FX 90Q, PS 100, and FX 200 spectrometers; ^1H spectra at 100 and 199.5 MHz, ^{31}P spectra at 36.2 MHz, and ^{11}B spectra at 28.7 and 64 MHz. Chemical shifts are relative to $SiMe_4$ (^1H), 85% H_3PO_4 (external) (^{31}P), and $BF_3{\cdot}OEt_2$ (external) (^{11}B), respectively. Infrared spectra were measured in Nujol mulls on a Perkin-Elmer 475 spectrophotometer. Melting points were measured in sealed, evacuated tubes. All experiments were carried out under dry oxygen-free nitrogen using Schlenk tube techniques. Solvents were dried and distilled under nitrogen prior to use. The compound $[Co(PEt_3)_4]$ was prepared by the procedure used to synthesize its less soluble PMe_3 analogue.[15] The precursors $[Pt_2(\mu\text{-cod})(PEt_3)_4]$,[5] $[Fe(cod)(\eta\text{-}C_5H_5)]$,[16] and $[FeH_2(2,3\text{-}Me_2\text{-}2,3\text{-}C_2B_4H_4)_2]$ [13] were made by literature methods.

Synthesis of $[CoFe(Me_4C_4B_8H_8)(PEt_3)_2]$ (1).—A solution of $[Co(PEt_3)_4]$ (0.53 g, 1 mmol) in pentane (6 cm^3) was added dropwise to $[FeH_2(2,3\text{-}Me_2\text{-}2,3\text{-}C_2B_4H_4)_2]$ (0.25 g, 0.96 mmol) in tetrahydrofuran (thf) (20 cm^3). Vigorous gas evolution commenced immediately. After 30 min stirring at room temperature, solvent was removed *in vacuo* and the residue dissolved in the minimum volume of thf (20 cm^3). This solution was poured on the top of an alumina column (3 × 2.5 cm) filled with pentane. Diethyl ether was then used to elute a dark brown solution. Reduction in volume of solvent, addition of pentane, and cooling to −20 °C afforded black *crystals* of $[CoFe(Me_4C_4B_8H_8)(PEt_3)_2]$ (1) (0.45 g, 81%) (Found: C, 43.4; H, 10.0. $C_{20}H_{50}B_8CoFeP_2$ requires C, 43.3; H, 9.1%); m.p. 155 °C, $\nu_{max.}$ (BH) at 2 539s, 2 509s, 2 497w, 2 487s, 2 476w, and 2 465s cm^{-1}. N.m.r. spectra: ^1H, δ 0.70 [d of t, 9 H, PCH_2Me, J(HH) 6.8, J(PH) 13.7], 0.98 [d of t, 9 H, PCH_2Me, J(HH) 6.6 Hz], 1.26 and 1.72 (m, 12 H, PCH_2Me), 1.75 (s, 3 H, MeC), 1.93 (s, 3 H, MeC), 1.99 (s, 3 H, MeC), and 2.25 p.p.m. (s, 3 H, MeC); $^{31}P\text{-}\{^1H\}$ (−70 °C), δ 36.4 [d, J(PP) 21] and 26.5 p.p.m. [d, J(PP) 21 Hz]; $^{11}B\text{-}\{^1H\}$, δ 78.0 (1 B), 49.1 (1 B), 8.3 (5 B), and −6.1 p.p.m. (1 B).

Molecular Structure Determination of (1).—Suitable crystals were obtained as described above. One crystal, *ca.* 0.04 × 0.03 × 0.03 cm, was sealed (epoxy-resin adhesive) inside a 0.05 cm diameter Lindemann tube under an atmosphere of nitrogen. Unit cell parameters and space group were determined, and intensity data measured, at 291 ± 1 K on a Nicolet *P*3 four-circle diffractometer following a procedure already described.[17]

Details pertinent to the present experiment were as follows: 15 reflections ($19.4 < 2\theta < 26.7°$) were taken from a rotation photograph and accurately centred in 2θ, ω, and χ; an orthorhombic unit cell was chosen by inspection of the lattice vectors and intervector cosines generated by the autoindexing program; rapid measurement of the diffracted intensities (0 0 1) to (5 5 5) indicated space group $P2_12_12_1$, subsequently confirmed by the successful structure solution and refinement; the singularity and quality of the crystal were authenticated by inspection of selected peak profiles; graphite-monochromated Mo-K_α *X*-radiation ($\lambda_{\alpha1}$ = 0.709 26, $\lambda_{\alpha2}$ = 0.713 54 Å) and a 96-step θ—2θ scan procedure were used (the 2θ scan rate being 0.048 83° s^{-1}) to collect one asymmetric unit of intensity data in the range $2.9 \leqslant 2\theta \leqslant 55.0°$; the intensities of the beams diffracted by the (4 0 $\bar{8}$) and (1 4 $\bar{5}$) planes were remeasured once every batch of 50 reflections, and their analysis [18] as individual functions of time subsequently revealed a *ca.* 17% decrease in intensity over the *ca.* 124 h of *X*-ray exposure. An exponential decay was best found to fit the data and a correction was applied; intensity data were adjusted for Lorentz and polarisation effects, but not for *X*-ray absorption. Of 3 833 measured intensities (excluding those systematically absent) 3 496 had $F \geqslant 2.0\sigma(F)$ and were retained for structure solution and refinement.

Crystal Data.—$C_{20}H_{50}B_8CoFeP_2$, *M* = 553.82, orthorhombic, space group $P2_12_12_1$, *a* = 16.533(5), *b* = 11.012(2), *c* = 16.279(3) Å, *U* = 2 963.7(12) Å^3, D_m not measured, *Z* = 4, D_c = 1.241 g cm^{-3}, *F*(000) = 1 172, μ(Mo-K_α) = 11.0 cm^{-1}.

Analysis of the Patterson synthesis revealed approximate positions of the metal atoms, the identities of which became apparent once light atoms were taken from subsequent difference electron density maps. Parallel full-matrix least-squares refinements of all non-H atoms with isotropic temperature factors converged at 0.077 and 0.073 for enantiomorphically related models, and all subsequent calculations refer to the latter. The F_o moduli were weighted according to $w^{-1} = [\sigma^2(F) + 0.005\,858\,F^2]$, a scheme that produced minimal variance as functions of sinθ and *F*. All non-hydrogen atoms were allowed anisotropic thermal motion. Methylene hydrogens (U_H * = 0.08 Å^2) were introduced into calculated positions and allowed to ride on their respective carbon atoms, and methyl functions were treated as rigid groups (see Appendix B) with U_H = 0.10 Å^2, each with C–H = 1.08 Å and H–C–H = 109.5°. Hydrogen atoms bonded directly to polyhedral atoms were located from difference-Fouriers and positionally refined (U_H = 0.06 Å^2).

Refinement converged at *R* 0.043 (*R'* 0.063) with a data : variable ratio better than 10 : 1. A final difference-Fourier showed no peak greater than 0.7, or trough less than −0.5 e Å^{-3}. Coefficients for analytical approximations to the atomic scattering factors were taken from ref. 19. Table 1 lists the derived fractional co-ordinates of non-hydrogen atoms. Appendix A containing the anisotropic thermal parameters, Appendix B the idealised H-atom co-ordinates, Appendix C which compares observed and calculated structure factor amplitudes, and Appendix D which gives the interconnectivity angles involving cage-H atoms of compound (1) are deposited in Supplementary Publication No. SUP 23329 (24 pp.).* Structure solution and refinement employed the SHELX76 crystallographic package [20]

TABLE 1

Atomic fractional co-ordinates * (× 10^5 Fe, Co, P; × 10^4 B, C; × 10^3 H) of refined atoms in [CoFe($Me_4C_4B_8H_8$)-(PEt_3)$_2$] (1)

Atom	*x*	*y*	*z*
Fe(1)	23 859(4)	−32 780(6)	19 366(4)
C(2)	1 623(3)	−4 268(5)	1 201(3)
C(3)	2 426(3)	−4 253(4)	854(3)
B(4)	2 779(3)	−2 943(5)	698(3)
Co(5)	19 910(4)	−15 980(5)	9 552(3)
B(6)	1 247(4)	−2 980(5)	1 354(3)
B(7)	1 765(3)	−3 256(5)	373(3)
C(2′)	2 486(3)	−4 391(5)	2 979(3)
C(3′)	3 271(3)	−4 273(5)	2 582(3)
B(4′)	3 541(4)	−2 915(5)	2 459(4)
B(5′)	2 799(4)	−2 106(5)	2 896(3)
B(6′)	2 112(4)	−3 149(6)	3 235(4)
B(7′)	3 141(4)	−3 353(6)	3 446(3)
B(cap)	1 688(4)	−1 833(5)	2 149(3)
C(201)	1 120(4)	−5 417(6)	1 248(5)
C(301)	2 824(4)	−5 378(5)	546(4)
C(201′)	2 177(4)	−5 618(5)	3 240(4)
C(301′)	3 816(4)	−5 331(6)	2 422(4)
P(1)	30 087(8)	−3 783(11)	5 740(8)
C(11)	3 180(3)	−155(6)	−535(3)
C(111)	3 435(6)	−1 250(8)	−1 022(4)
C(12)	4 028(3)	−711(5)	969(4)
C(121)	4 703(4)	119(9)	724(6)
C(13)	2 900(4)	1 222(5)	897(4)
C(131)	2 838(8)	1 395(7)	1 820(6)
P(2)	9 265(7)	−6 239(12)	3 959(8)
C(21)	388(4)	−1 482(6)	−395(4)
C(211)	834(6)	−1 531(8)	−1 215(5)
C(22)	1 017(4)	875(5)	−102(5)
C(221)	248(4)	1 439(7)	−447(6)
C(23)	103(4)	−319(7)	1 134(4)
C(231)	303(6)	711(10)	1 734(5)
H(4)	322(4)	−282(7)	42(4)
H(6)	63(5)	−303(7)	153(4)
H(7)	146(4)	−349(7)	−23(5)
H(4′)	413(5)	−272(7)	230(4)
H(5′)	264(4)	−129(7)	299(5)
H(6′)	155(4)	−324(7)	360(4)
H(7′)	348(4)	−347(6)	405(4)
H(cap)	123(4)	−152(7)	256(4)

* Estimated standard deviations in parentheses throughout this paper.

implemented on the CDC 7600 computer of the University of London Computer Centre. Least-squares planes were analysed using XANADU [21] and plots constructed *via* ORTEP-II.[22]

Synthesis of [FePt($Me_4C_4B_8H_8$)(PEt_3)$_2$] (2).—A pentane (15 cm^3) solution of [Pt_2(μ-cod)(PEt_3)$_4$] (0.28 g, 0.29 mmol) was treated with a pentane (5 cm^3) solution of [FeH_2-(2,3-Me_2-2,3-$C_2B_4H_4$)$_2$] (0.15 g, 0.58 mmol) and the mixture stirred (5 h) at room temperature. No gas evolution was observed, but the colour changed to dark red and solid precipitated. Solvent was removed *in vacuo* and the residue chromatographed on alumina. Two bands developed, and these were eluted with diethyl ether and thf, respectively.

* The isotropic thermal parameter is defined as exp{$-8\pi^2U\sin^2\theta/\lambda^2$}.

† For details see Notices to Authors No. 7, *J. Chem. Soc., Dalton Trans.*, 1981, Index issue.

The first fraction on reduction in volume and cooling to −20 °C gave dark green *crystals* of [$FePt(Me_4C_4B_8H_8)(PEt_3)_2$] (2) (0.21 g, 52%) (Found: C, 35.4; H, 8.1. $C_{20}H_{50}B_8FeP_2Pt$ requires C, 34.8; H, 7.5%); m.p. 158 °C, $\nu_{max.}$ (BH) at 2 533s, 2 512s, 2 495s, and 2 468w cm^{-1}. N.m.r. spectra: ^1H, δ 0.80 [d of t, 18 H, PCH_2Me, J(HH) 7, J(PH) 16 Hz], 1.71 (m, 12 H, PCH_2Me), 1.93 (s, 6 H, MeC), and 2.14 p.p.m. (s, 6 H, MeC); ^{31}P-{^1H}, δ −1.7 p.p.m. [J(PtP) 2 871 Hz]; ^{31}P-{^1H} (−90 °C), δ 3.0 [J(PtP) 3 135] and −4.3 p.p.m. [J(PtP) 2 607 Hz], both signals too broad to measure J(PP); ^{11}B-{^1H} ([$^2H_6$]benzene–PhMe), δ 15.5 (1 B), 10.6 (3 B), 0.03 (3 B), and −11.3 p.p.m. (1 B).

The second fraction, red in colour, was identified *via* ^1H and ^{31}P n.m.r. spectroscopy as a mixture of [$FeH_2(2,3\text{-}Me_2\text{-}2,3\text{-}C_2B_4H_4)_2$], *trans*-[$PtH_2(PEt_3)_2$], and [$Pt(PEt_3)_3$], the last two presumably formed by reaction of [$Pt_2(\mu\text{-cod})(PEt_3)_4$] with hydrogen and free triethylphosphine.

Unit Cell and Space Group Determination of Compound (2).—A small single crystal of (2), recrystallised from diethyl ether, was sealed in a Lindemann tube under dry nitrogen and set on the $P3$ diffractomer. Unit cell dimensions were determined, *via* the centring of 15 reflections in the range $19.9 \leqslant 2\theta \leqslant 28.7°$ (Mo-K_α X-radiation), to be (at 291 ± 1 K) $a = 16.883(4)$, $b = 11.144(4)$, $c = 16.196(5)$ Å, $\alpha = \beta = \gamma = 90° \pm 2\sigma$. Partial rotation photographs (Polaroid cassette) about each of the three axes indicated the Laue symmetry to be $m\ m\ m$, and rapid collection of the reflection intensities for (0 0 1) to (5 5 5) suggested systematic absences consistent with the space group $P2_12_12_1$. Thus (2) is probably * isostructural with (1). Full three-dimensional intensity data were not collected.

Synthesis of [$Fe_2(Me_4C_4B_8H_8)(\eta\text{-}C_5H_5)$].—A solution of [$FeH_2(2,3\text{-}Me_2\text{-}2,3\text{-}C_2B_4H_4)_2$] (0.25 g, 0.94 mmol) in pentane (15 cm^3) was added to a pentane solution (10 cm^3) of [Fe(cod)(η-C_5H_5)] (0.24 g, 1 mmol). After stirring (20 h) at room temperature, the volatile material was removed *in vacuo* and the residue dissolved in thf and filtered through Celite. Reduction in volume of the solution *in vacuo* and cooling to −20 °C afforded dark brown *crystals* of [$Fe_2(Me_4C_4B_8H_8)(\eta\text{-}C_5H_5)$] (3) (0.23 g, 61%) (Found: C, 40.3; H, 7.0%; M, 381 (mass spectrum). $C_{13}H_{25}B_8Fe_2$ requires C, 41.1; H, 6.6%; M, 381); $\nu_{max.}$ (BH) at 2 591s, 2 576s, 2 557s, and 2 523m cm^{-1}; ^{11}B-{^1H} n.m.r. ([$^2H_1$]chloroform), δ 81.3 (1 B), −4.9 (3 B), −118.2 (3 B), and −197.5 p.p.m. (1 B).

Microscopic examination of compound (3) showed the crystals to be ill formed and partially opaque. Several single crystals, mounted under dry nitrogen in Lindemann tubes, were photographed (Weissenberg camera), but diffracted so poorly that the unit cell and space group could not be established. Recrystallisations from a variety of other solvents afforded no improvement in crystal quality.

DISCUSSION

As described above, the compounds [$Co(PEt_3)_4$] and [$FeH_2(2,3\text{-}Me_2\text{-}2,3\text{-}C_2B_4H_4)_2$] react at room temperature in pentane with gas evolution to give a black crystalline complex formulated as [$CoFe(Me_4C_4B_8H_8)(PEt_3)_2$] (1) on the basis of microanalysis and spectroscopic properties. The related reaction of [$FeH_2(2,3\text{-}Me_2\text{-}2,3\text{-}C_2B_4H_4)_2$] with [$Pt_2(\mu\text{-cod})(PEt_3)_4$] did not lead to release of hydrogen but *trans*-[$PtH_2(PEt_3)_2$] and [$Pt(PEt_3)_3$] were formed together with a green complex [$FePt(Me_4C_4B_8H_8)(PEt_3)_2$] (2), isostructural with (1). A further example of this family [12] of complexes, [$Fe_2(Me_4C_4B_8H_8)(\eta\text{-}C_5H_5)$] (3), was obtained by reacting [Fe(cod)(η-C_5H_5)] with the dihydridoiron compound. The reactions observed are summarised in the accompanying Scheme.

TABLE 2

Interatomic distances (Å) in [$CoFe(Me_4C_4B_8H_8)(PEt_3)_2$] (1)

(*a*) Polyhedron			
Fe(1)–C(2)	2.053(5)	Fe(1)–C(2′)	2.100(5)
Fe(1)–C(3)	2.064(5)	Fe(1)–C(3′)	2.108(5)
Fe(1)–B(4)	2.151(5)	Fe(1)–B(4′)	2.128(6)
Fe(1)–Co(5)	2.530 0(8)	Fe(1)–B(5′)	2.137(6)
Fe(1)–B(6)	2.134(6)	Fe(1)–B(6′)	2.166(6)
C(2)–C(3)	1.443(8)	C(2′)–C(3′)	1.456(7)
C(3)–B(4)	1.577(7)	C(3′)–B(4′)	1.573(8)
B(4)–Co(5)	2.017(5)	B(4′)–B(5′)	1.674(9)
Co(5)–B(6)	2.062(6)	B(5′)–B(6′)	1.706(9)
B(6)–C(2)	1.568(8)	B(6′)–C(2′)	1.557(8)
C(2)–B(7)	1.764(7)	C(2′)–B(7′)	1.748(8)
C(3)–B(7)	1.735(7)	C(3′)–B(7′)	1.746(8)
B(4)–B(7)	1.790(8)	B(4′)–B(7′)	1.802(8)
Co(5)–B(7)	2.090(6)	B(5′)–B(7′)	1.734(9)
B(6)–B(7)	1.838(8)	B(6′)–B(7′)	1.750(9)
Co(5)–B(cap)	2.024(6)	B(5′)–B(cap)	2.223(9)
B(6)–B(cap)	1.949(8)	B(6′)–B(cap)	2.391(8)
Fe(1)–B(cap)	1.996(6)		
(*b*) Exo-polyhedron			
C(2)–C(201)	1.516(7)	C(2′)–C(201′)	1.505(7)
C(3)–C(301)	1.490(7)	C(3′)–C(301′)	1.497(8)
B(4)–H(4)	0.87(7)	B(4′)–H(4′)	1.04(8)
Co(5)–P(1)	2.240 5(14)	B(5′)–H(5′)	0.96(8)
Co(5)–P(2)	2.253 2(14)	B(6′)–H(6′)	1.11(7)
B(6)–H(6)	1.06(7)	B(7′)–H(7′)	1.13(7)
B(7)–H(7)	1.14(7)	B(cap)–H(cap)	1.06(7)
(*c*) Phosphine ligands			
P(1)–C(11)	1.844(5)	P(2)–C(21)	1.828(6)
P(1)–C(12)	1.840(5)	P(2)–C(22)	1.845(6)
P(1)–C(13)	1.847(5)	P(2)–C(23)	1.846(6)
C(11)–C(111)	1.504(10)	C(21)–C(211)	1.527(11)
C(12)–C(121)	1.498(8)	C(22)–C(221)	1.523(9)
C(13)–C(131)	1.518(11)	C(23)–C(231)	1.533(12)

A single crystal X-ray diffraction study of complex (1) established the structure shown in Figure 1, which presents a perspective view of a single molecule and shows the atomic numbering scheme. Hydrogen atoms are not included in this Figure, but their numbering is described in footnote *a* of Table 6. Table 2 lists internuclear distances, and Table 3 interconnectivity angles [apart from those involving cage-H atoms, which appear in Appendix D (see SUP No. 23329)].

Compound (1) crystallises as discrete molecules with no serious intermolecular contacts. In basic architecture it closely resembles that of the compound [$CoFe(Me_4C_4B_8H_8)(\eta\text{-}C_5H_5)$] (4) [12] except, of course, that the two PEt_3 functions of (1) replace the cyclopentadienyl ligand of (4). The difference of one unit between the formal oxidation states of cobalt in these two species is reflected in differences in the lengths of a number of cage connectivities, as will be subsequently discussed. Compounds (1), (2) [presumably isostructural with (1)], (4),

* We have recently experienced chemical analogues crystallising in the same space group with very similar cell dimensions that are not fully isostructural (ref. 10).

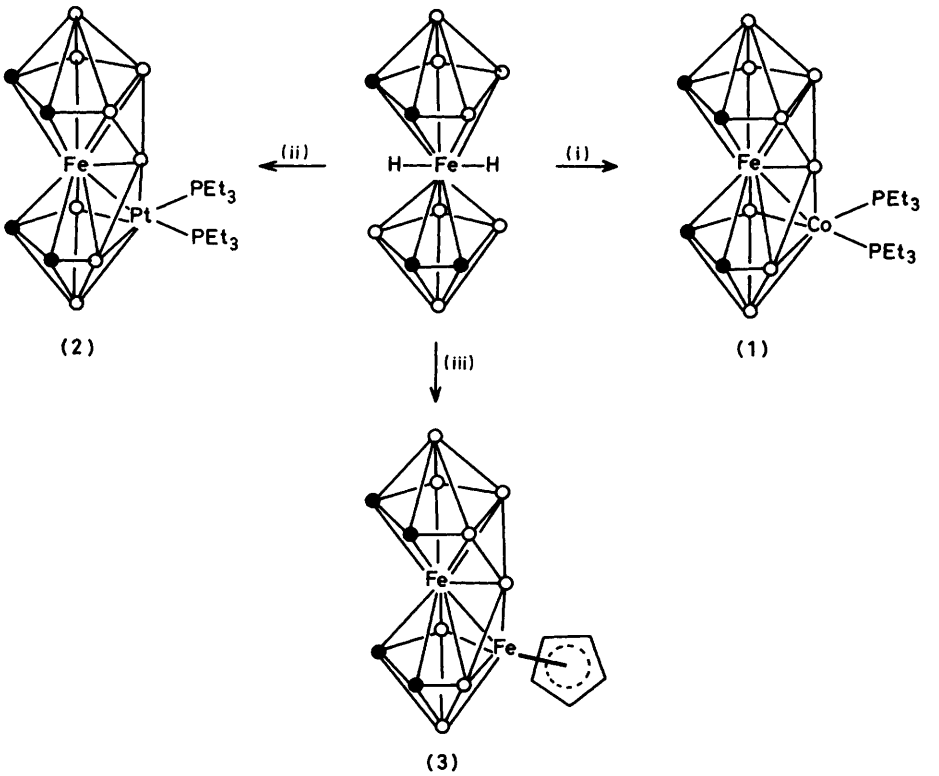

SCHEME (i) $[Co(PEt_3)_4]$; (ii) $[Pt_2(\mu\text{-cod})(PEt_3)_4]$; (iii) $[Fe(cod)(\eta\text{-}C_5H_5)]$; (●) = CMe, (○) = BH

and (3) [presumably isostructural with (4)] represent members of a potentially large family of carbadimetallaboranes that may in principle be formed by direct insertion of low-valent metal fragments into ' sandwich ' carbametallaboranes.

The polyhedral geometry of (1) involves two *closo*-pentagonal bipyramids joined at a common apical vertex (the Fe^{II} atom). The inserted Co^{II} atom occupies an equatorial site (as part of a CoBBCC belt) in one of the bipyramids, and the two cages are further fused by a double-capping BH function, which bridges FeCoB and FeBB deltahedra. When viewed along their common axis [B(7)Fe(1)B(7')] the conformation of the two bipyramids is closely eclipsed.

Grimes and co-workers [12] have rationalised the cage architecture of (4) in terms of the total number of polyhedral skeletal electron pairs (p.s.e.p.) available to the cluster, by use of p.s.e.p. theory [23] and the capping principle.[24] We shall not fully restate the arguments but merely concur that the 16 p.s.e.p. of compounds (1)—(4) are only sufficient to occupy the bonding molecular orbitals of two fused *closo*-seven atom polyhedra (*i.e.* necessitate one capping atom). Moreover, recent extended-Hückel molecular orbital calculations [25] have shown that the most stable conformation of the model compound $[Fe(BH)(B_6H_6)_2]^{4-}$ is that in which the capping BH occupies a double-capping or wedge position. In recognition of the fact that such species possess even fewer bonding electrons than a molecule comprising fused *closo*-seven and -eight atom heteroborane cages, which would be electron deficient in the normal sense, compound (4) has been termed ' electron hyper-deficient.'

Two extensions of the application of electron counting principles to these compounds have been proposed.[12] Reduction in the number of p.s.e.p. (in the first instance to 15) should increase to two the number of capping units, generating a fused pentagonal bipyramid and octahedron, in which the common iron atom would be partially encapsulated in a heteroborane framework. However, since the number of p.s.e.p. provided by the BH and CMe functions is unalterable, this would necessarily involve reduction from four to two in the number of electrons provided by the two metal atoms, and it is difficult to envisage a system in which this would be the case.

Conversely, increasing the number of p.s.e.p. (in the first instance to 17) would eradicate the need for capping and produce a molecule with fused seven and eight atom polyhedra. In theory the p.s.e.p. count would be increased by higher oxidation states for one or both metal atoms (although it is difficult to conceive of the inserted metal furnishing more than two electrons for cage bonding) and/or the presence of face-bridging H atoms. Thus, whilst $[Fe^{II}H_2(2,3\text{-}Me_2\text{-}2,3\text{-}C_2B_4H_4)_2]$ loses both μ-H atoms on forming compounds (1)—(4), the higher metal oxidation state in $[Co^{III}H(2,3\text{-}Me_2\text{-}2,3\text{-}C_2B_4H_4)_2]$ may encourage hydrogen retention under favourable circumstances. However, Grimes and co-workers [26] have found that $[CoH(2,3\text{-}Me_2\text{-}2,3\text{-}C_2B_4H_4)_2]$ reacts with $[Co(CO)_2(\eta\text{-}C_5H_5)]$ in refluxing thf or under u.v. irradi-

TABLE 3

Interconnectivity angles (°) in $[CoFe(Me_4C_4B_8H_8)(PEt_3)_2]$ (1)

(*a*) Polyhedral surface

C(2)–Fe(1)–C(3)	41.0(2)	C(2′)–Fe(1)–C(3′)	40.5(2)
C(3)–Fe(1)–B(4)	43.9(2)	C(3′)–Fe(1)–B(4′)	43.6(2)
B(4)–Fe(1)–Co(5)	50.24(14)	B(4′)–Fe(1)–B(5′)	46.2(2)
Co(5)–Fe(1)–B(6)	51.62(15)	B(5′)–Fe(1)–B(6′)	46.7(2)
B(6)–Fe(1)–C(2)	43.9(2)	B(6′)–Fe(1)–C(2′)	42.8(2)
Fe(1)–C(2)–B(6)	70.8(3)	Fe(1)–C(2′)–B(6′)	70.9(3)
Fe(1)–C(2)–C(3)	69.9(3)	Fe(1)–C(2′)–C(3′)	70.0(3)
Fe(1)–C(3)–C(2)	69.1(3)	Fe(1)–C(3′)–C(2′)	69.5(3)
Fe(1)–C(3)–B(4)	71.0(3)	Fe(1)–C(3′)–B(4′)	68.9(3)
Fe(1)–B(4)–C(3)	65.1(3)	Fe(1)–B(4′)–C(3′)	67.5(3)
Fe(1)–B(4)–Co(5)	74.7(2)	Fe(1)–B(4′)–B(5′)	67.2(3)
Fe(1)–Co(5)–B(4)	55.1(2)	Fe(1)–B(5′)–B(4′)	66.6(3)
Fe(1)–Co(5)–B(6)	54.2(2)	Fe(1)–B(5′)–B(6′)	67.5(3)
Fe(1)–B(6)–Co(5)	74.2(2)	Fe(1)–B(6′)–B(5′)	65.8(3)
Fe(1)–B(6)–C(2)	65.3(3)	Fe(1)–B(6′)–C(2′)	66.4(3)
C(2)–B(7)–C(3)	48.7(3)	C(2′)–B(7′)–C(3′)	49.3(3)
C(3)–B(7)–B(4)	53.1(3)	C(3′)–B(7′)–B(4′)	52.6(3)
B(4)–B(7)–Co(5)	62.1(2)	B(4′)–B(7′)–B(5′)	56.5(3)
Co(5)–B(7)–B(6)	62.9(2)	B(5′)–B(7′)–B(6′)	58.6(4)
B(6)–B(7)–C(2)	51.6(3)	B(6′)–B(7′)–C(2′)	52.9(3)
B(cap)–Fe(1)–B(6)	56.2(2)	B(cap)–Fe(1)–B(6′)	70.0(2)
Fe(1)–B(6)–B(cap)	58.3(2)	Fe(1)–B(6′)–B(cap)	51.7(2)
B(6)–B(cap)–Fe(1)	65.5(3)	B(6′)–B(cap)–Fe(1)	58.3(2)
B(cap)–B(6)–Co(5)	60.5(2)	B(cap)–B(6′)–B(5′)	63.2(3)
B(6)–Co(5)–B(cap)	57.0(2)	B(6′)–B(5′)–B(cap)	73.6(4)
Co(5)–B(cap)–B(6)	62.5(2)	B(5′)–B(cap)–B(6′)	43.2(2)
B(cap)–Fe(1)–Co(5)	51.48(14)	B(cap)–Fe(1)–B(5′)	65.0(2)
Fe(1)–Co(5)–B(cap)	50.5(2)	Fe(1)–B(5′)–B(cap)	54.4(2)
Co(5)–B(cap)–Fe(1)	78.0(2)	B(5′)–B(cap)–Fe(1)	60.6(2)
Co(5)–B(cap)–B(5′)	109.7(3)	B(6′)–B(cap)–B(6)	102.0(3)

(*b*) Exo-polyhedron *

C(201)–C(2)–Fe(1)	138.6(4)	C(201′)–C(2′)–Fe(1)	136.5(4)
C(201)–C(2)–C(3)	122.2(5)	C(201′)–C(2′)–C(3′)	120.5(5)
C(201)–C(2)–B(7)	129.7(5)	C(201′)–C(2′)–B(7′)	132.4(4)
C(201)–C(2)–B(6)	122.0(5)	C(201′)–C(2′)–B(6′)	125.4(5)
C(301)–C(3)–Fe(1)	137.2(4)	C(301′)–C(3′)–Fe(1)	137.4(4)
C(301)–C(3)–C(2)	121.9(5)	C(301′)–C(3′)–C(2′)	123.0(5)
C(301)–C(3)–B(7)	130.7(4)	C(301′)–C(3′)–B(7′)	131.8(5)
C(301)–C(3)–B(4)	122.8(5)	C(301′)–C(3′)–B(4′)	123.2(5)
P(1)–Co(5)–Fe(1)	114.80(5)	P(2)–Co(5)–Fe(1)	143.59(5)
P(1)–Co(5)–B(6)	167.9(2)	P(2)–Co(5)–B(6)	90.7(2)
P(1)–Co(5)–B(7)	122.1(2)	P(2)–Co(5)–B(7)	95.4(2)
P(1)–Co(5)–B(4)	84.1(2)	P(2)–Co(5)–B(4)	140.4(2)
P(1)–Co(5)–B(cap)	121.9(2)	P(2)–Co(5)–B(cap)	104.8(2)
P(1)–Co(5)–P(2)	100.91(5)		

(*c*) Phosphine ligands

Co(5)–P(1)–C(11)	117.8(2)	Co(5)–P(2)–C(21)	114.7(2)
Co(5)–P(1)–C(12)	118.1(2)	Co(5)–P(2)–C(22)	122.7(2)
Co(5)–P(1)–C(13)	114.8(2)	Co(5)–P(2)–C(23)	113.6(2)
C(11)–P(1)–C(12)	103.2(3)	C(21)–P(2)–C(22)	101.1(3)
C(11)–P(1)–C(13)	99.6(3)	C(21)–P(2)–C(23)	101.2(3)
C(12)–P(1)–C(13)	100.3(3)	C(22)–P(2)–C(23)	100.5(3)
P(1)–C(11)–C(111)	116.9(5)	P(2)–C(21)–C(211)	113.5(5)
P(1)–C(12)–C(121)	117.9(5)	P(2)–C(22)–C(221)	117.3(5)
P(1)–C(13)–C(131)	114.1(5)	P(2)–C(23)–C(231)	113.0(6)

* Angles involving the cage hydrogen atoms have been deposited (as Appendix D SUP No. 23329).

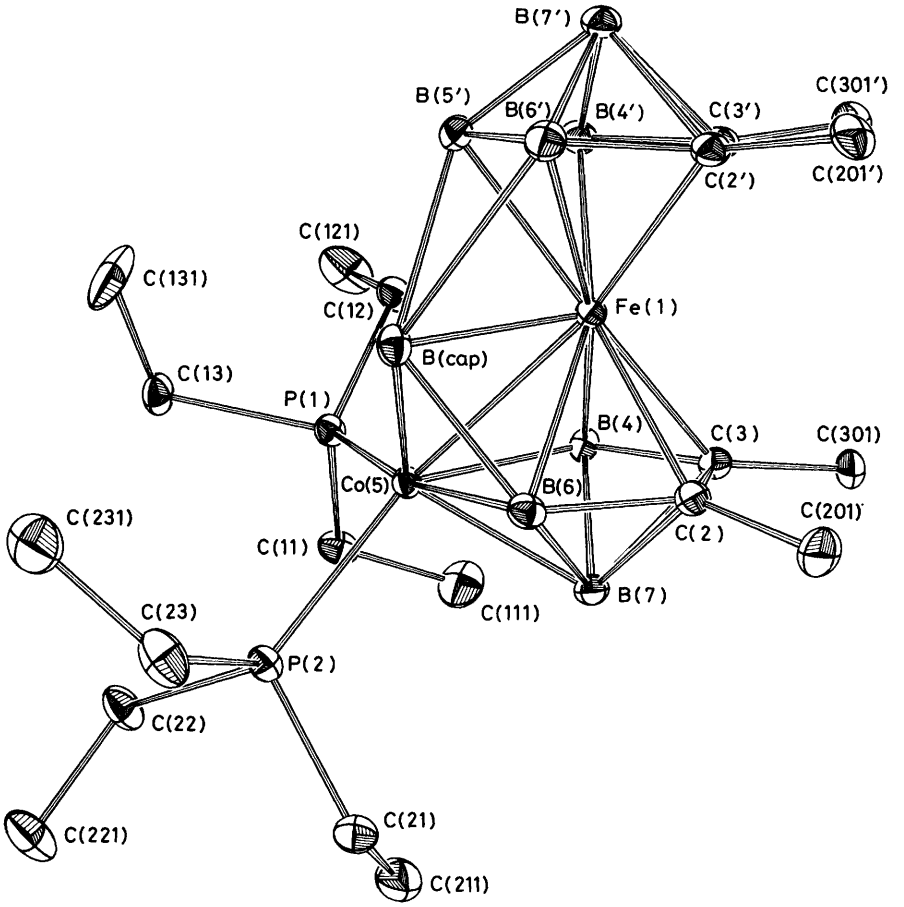

FIGURE 1 Molecular structure of $[CoFe(Me_4C_4B_8H_8)(PEt_3)_2]$ (1) with hydrogen atoms omitted for clarity. Thermal ellipsoids are constructed at the 30% electron probability level

ation [the same technique employed to insert $Co(\eta\text{-}C_5H_5)$ into the iron dihydride to produce (4)] to afford a complex mixture of di- and tri-cobalt species all of which involve some cage degradation with loss of a BH function. The insertion of ML_2 (M = Ni, Pd, or Pt; L = PR_3 or CNR, where R = alkyl or aryl) or $Fe(\eta\text{-}C_5H_5)$ fragments into $[CoH(2,3\text{-}Me_2\text{-}2,3\text{-}C_2B_4H_4)_2]$ under the mild conditions described herein has yet to be examined. In addition, direct insertion into 'sandwich' molecules in which the metal is formally present in the +4 oxidation state, where there are no μ-H functions that may be lost, *e.g.* $[Ni(2,3\text{-}C_2B_9H_{11})_2]$,[27] may be fruitful.

Comparison of the molecular structures of (1) and (4) reveals that the major differences involve atoms Co(5) and B(cap). As detailed in Table 4, all connectivities including these atoms, *except the Co(5)–B(cap) link itself*, are significantly larger in (1). For the bonds involving the metal this change is understandable in terms of the greater polyhedral radius of Co^{II} in (1) over Co^{III} in (4). The reduction in the Co(5)–B(cap) length in (1), 0.033(9) Å, is just statistically significant and results in a capping atom that lies *ca.* 0.39 Å closer to the mean plane through the lower equatorial belt than to that through the upper belt [Table 5(*b*)]. A similar but less serious asymmetry occurs in (4) [12] and its origin has been traced to the influence of the cobalt atom upon the cage molecular orbitals.[25]

TABLE 4

Comparison of selected molecular parameters of compounds $[CoFe(Me_4C_4B_8H_8)(PEt_3)_2]$ (1) and $[CoFe(Me_4C_4B_8H_8)(\eta\text{-}C_5H_5)]$ (4)

Parameter	(1)	(4) [a]	Difference
Co(5)–Fe(1)	2.530 0(8)	2.480(1)	0.050(13) [b]
Co(5)–B(4)	2.017(5)	1.935(7)	0.082(9)
Co(5)–B(6)	2.062(6)	1.953(7)	0.109(9)
Co(5)–B(7)	2.090(6)	1.997(8)	0.093(10)
Co(5)–B(cap)	2.024(6)	2.057(7)	0.033(9)
B(cap)–Fe(1)	1.996(6)	1.912(7)	0.084(9)
B(cap)–B(6)	1.949(8)	1.86(1)	0.079(13)
B(cap)–B(5')	2.223(9)	2.10(1)	0.123(13)
B(cap)–B(6')	2.391(8)	2.19(1)	0.201(13)

[a] Taken from ref. 12. Some atoms have been renumbered for consistency with (1). [b] E.s.d. of the difference between two like parameters i and j given by $(\sigma_i^2 + \sigma_j^2)^{\frac{1}{2}}$.

The equatorial belts of the two pentagonal bipyramids of (1) are essentially parallel (dihedral angle 6.9°), and an average of 3.250 Å apart. Given that the CMe functions are eclipsed with respect to the polyhedral axis, and that equatorial substituents to a pentagonal bipyramid

TABLE 5

Least-squares planes data for the compound $[CoFe(Me_4C_4B_8H_8)(PEt_3)_2]$ (1)

(*a*) Coefficients (*P*, *Q*, *R*, and *S*) where the plane is defined by the expression $Px + Qy + Rz = S$, Å, in which *x*, *y*, and *z* are the atomic fractional co-ordinates

	P	*Q*	*R*	*S*
Plane 1: C(2), C(3), B(4), Co(5), B(6)	6.426	0.434	14.985	2.672
Plane 2: C(2′), C(3′), B(4′), B(5′), B(6′)	7.752	−0.456	14.362	6.421
Plane 3: Co(5), P(1), P(2)	−1.858	5.829	13.689	0.006

(*b*) Individual atomic deviations (Å) from the planes

Plane 1		Plane 2	
C(2)	−0.014	C(2′)	−0.015
C(3)	−0.017	C(3′)	0.017
B(4)	0.032	B(4′)	−0.012
Co(5)	−0.030	B(5′)	0.003
B(6)	0.030	B(6′)	0.006
Fe(1)	1.622	Fe(1)	−1.641
B(7)	−1.119	B(7′)	1.115
B(cap)	1.554	B(cap)	−1.943
C(201)	−0.316	C(201′)	0.176
C(301)	−0.271	C(301′)	0.258
H(4)	−0.099	H(4′)	0.209
H(6)	−0.109	H(5′)	−0.016
		H(6′)	0.103

(*c*) Dihedral angles (°): 1—2 6.9; 1—3 41.3; 2—3 48.1

ideally radiate at elevation angles of 0°, inter-annular close contacts between methyl groups (van der Waals radius ~2.0 Å) occur.

In (1) some relief from this crowding is gained by both pairs of methyl carbon atoms bending out of their respective equatorial planes by 6.7—12.0°, distortions

TABLE 6

Interligand H · · · H contacts ≤2.3 Å in the compound $[CoFe(Me_4C_4B_8H_8)(PEt_3)_2]$ (1) [a]

(*a*) Intramolecular

(i)	H(202) · · · H(203′)	2.293
(ii)	H(303) · · · H(302′)	2.057
(iii)	H(4) · · · H(12)	2.153
(iv)	H(7) · · · H(210)	2.251
(v)	H(110) · · · H(22)	2.089
(vi)	H(13) · · · H(220)	1.875

(*b*) Intermolecular [b]

H(201′) · · · H(230^{I})	2.269
H(303) · · · H(131^{II})	2.282
H(131) · · · H($203'^{III}$)	2.266

[a] H(*i*) is a cage hydrogen atom bound to B(*i*). H(*i*0*k*) or H(*i*0*k*′) is a cage methyl hydrogen bonded to C(*i*01) or C(*i*01′) respectively. H(*ij*) and H(*ij*0) are methylene H atoms on C(*ij*), whilst H(*ijk*) are methyl H atoms bonded to C(*ij*1). [b] Roman numeral superscripts denote the following equivalent positions, relative to the reference molecule at *x*, *y*, *z*; I $-x$, $y - \frac{1}{2}$, $\frac{1}{2} - z$; II *x*, $y - 1$, *z*; III *x*, $1 + y$, *z*.

clearly visible in Figure 1. Nevertheless, two inter-annular H · · · H contacts <2.3 Å still exist, listed as contacts (i) and (ii) of Table 6(*a*). Contacts (iii) and (iv) of this Table are CH_2–H · · · cage–H interactions, but rather more serious are contacts (v) and (vi), the CH_2–H · · · CH_2–H interactions that are inevitable consequences of the ' type 1 ' stereochemistry of the *cis*-$[Co(PEt_3)_2]$ fragment (see Figure 5 of ref. 1). The relatively small P–Co–P angle [100.91(5)°] and relatively large Co(5)–P(2)–C(22) angle [122.7(2)°] are totally consistent with the stereochemistry adopted.

A crystal packing diagram, projected onto the (0 1 0) face, is presented in Figure 2, and the three intermolecular contacts <2.3 Å that occur in the lattice are given in Table 6(*b*). Generally, though, the crystalline array is free from any serious intermolecular crowding.

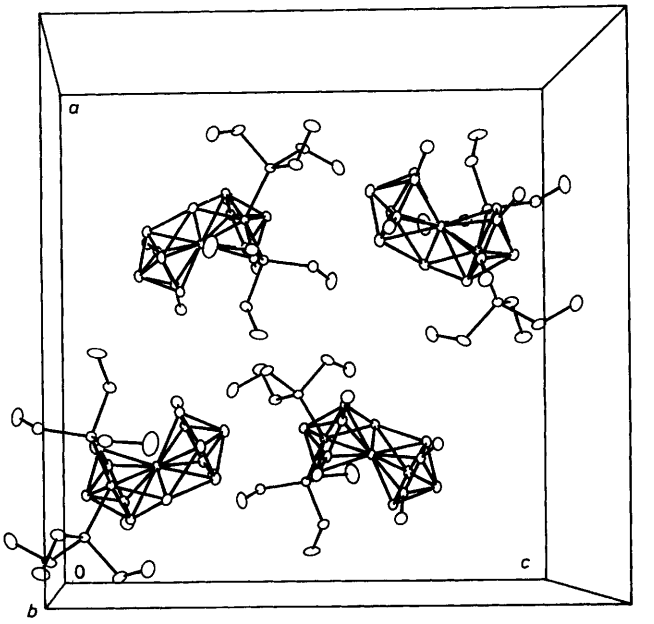

FIGURE 2 Unit cell contents of $[CoFe(Me_4C_4B_8H_8)(PEt_3)_2]$ (1) with hydrogens omitted

We thank the S.E.R.C. for support.

[2/033 *Received*, 8*th January*, 1982]

REFERENCES

[1] Part 11, G. K. Barker, M. Green, F. G. A. Stone, and A. J. Welch, *J. Chem. Soc., Dalton Trans.*, 1980, 1186.
[2] M. Green, J. L. Spencer, F. G. A. Stone, and A. J. Welch, *J. Chem. Soc., Dalton Trans.*, 1975, 179.
[3] W. E. Carroll, M. Green, F. G. A. Stone, and A. J. Welch, *J. Chem. Soc., Dalton Trans.*, 1975, 2263.

[4] M. Green, J. L. Spencer, and F. G. A. Stone, *J. Chem. Soc., Dalton Trans.*, 1979, 1679.
[5] G. K. Barker, M. Green, F. G. A. Stone, A. J. Welch, T. P. Onak, and G. Siwapanyoyos, *J. Chem. Soc., Dalton Trans.*, 1979, 1687.
[6] G. K. Barker, M. Green, F. G. A. Stone, A. J. Welch, and W. C. Wolsey, *J. Chem. Soc., Chem. Commun.*, 1980, 627.
[7] M. Green, J. A. K. Howard, J. L. Spencer, and F. G. A. Stone, *J. Chem. Soc., Dalton Trans.*, 1975, 2274.
[8] G. K. Barker, M. Green, M. P. Garcia, F. G. A. Stone, J-M. Bassett, and A. J. Welch, *J. Chem. Soc., Chem. Commun.*, 1980, 1266.
[9] G. K. Barker, M. P. Garcia, M. Green, G. N. Pain, F. G. A. Stone, S. K. R. Jones, and A. J. Welch, *J. Chem. Soc., Chem. Commun.*, 1981, 652.
[10] G. K. Barker, M. P. Garcia, M. Green, F. G. A. Stone, J-M. Bassett, and A. J. Welch, *J. Chem. Soc., Chem. Commun.*, 1981, 653.
[11] M. P. Garcia, M. Green, F. G. A. Stone, R. G. Somerville, and A. J. Welch, *J. Chem. Soc., Chem. Commun.*, 1981, 871.
[12] W. M. Maxwell, E. Sinn, and R. N. Grimes, *J. Am. Chem. Soc.*, 1976, **98**, 3490.
[13] W. M. Maxwell, V. R. Miller, and R. N. Grimes, *Inorg. Chem.*, 1976, **15**, 1343.
[14] J. R. Pipal and R. N. Grimes, *Inorg. Chem.*, 1979, **18**, 263.
[15] H. F. Klein, *Angew. Chem., Int. Ed. Engl.*, 1980, **19**, 362.
[16] K. Jonas, *Adv. Organomet. Chem.*, 1981, **19**, 97; K. Jonas and L. Schieferstein, *Angew. Chem., Int. Ed. Engl.*, 1979, **18**, 549; L. Schieferstein, Dissertation, Ruhr-Universitat Bochum, 1978.
[17] A. G. Modinos and P. Woodward, *J. Chem. Soc., Dalton Trans.*, 1974, 2065.
[18] A. G. Modinos, 'DRSYN,' a Fortran program for data analysis.
[19] 'International Tables for *X*-Ray Crystallography,' Kynoch Press, Birmingham, 1974, vol. 4.
[20] G. M. Sheldrick, 'SHELX76,' University Chemical Laboratory, Cambridge, 1976.
[21] G. M. Sheldrick and P. Roberts, 'XANADU,' University Chemical Laboratory, Cambridge, 1976.
[22] C. K. Johnson, 'ORTEP-II,' Report ORNL-5138, Oak Ridge National Laboratory, Tennessee, 1976.
[23] K. Wade, *Chem. Commun.*, 1971, 792; *Adv. Inorg. Chem. Radiochem.*, 1976, **18**, 1; R. N. Grimes, *Ann. N.Y. Acad Sci.*, 1974, **239**, 180; R. Mason and D. M. P. Mingos, *M.T.P. Internat. Rev. Sci. Phys. Sci. Ser. 2*, 1975, **11**, 121; R. W. Rudolph, *Acc. Chem. Res.*, 1976, **9**, 446.
[24] D. M. P. Mingos, *Nature Phys. Sci.*, 1972, **236**, 99.
[25] M. J. Calhorda and D. M. P. Mingos, *J. Organomet. Chem.*, 1982, **229**, 229.
[26] W. M. Maxwell, V. R. Miller, and R. N. Grimes, *J. Am. Chem. Soc.*, 1976, **98**, 4818.
[27] M. F. Hawthorne, D. C. Young, T. D. Andrews, D. V. Howe, R. L. Pilling, A. D. Pitts, M. Reintjes, L. F. Warren, and P. A. Wegner, *J. Am. Chem. Soc.*, 1968, **90**, 879; D. St.Clair, A. Zalkin, and D. H. Templeton, *ibid.*, 1970, **92**, 1173.